Journal of Cellular Automata, Vol. 12, pp. 309–332
Reprints available directly from the publisher
Photocopying permitted by license only

VALANCA: A Cellular Automata Model for Simulating Snow Avalanches

MARIA VITTORIA AVOLIO[1,*], ALESSIA ERRERA[2], VALERIA LUPIANO[3], PAOLO MAZZANTI[4] AND SALVATORE DI GREGORIO[1]

[1]*Department of Mathematics & Center of High-Performance Computing, University of Calabria, Arcavacata, 87036, Rende (CS), Italy*

[2]*Eni s.p.a., exploration & production division, via Emilia 1, 20097, San Donato Milanese (MI), Italy*

[3]*Department of Earth Sciences, University of Calabria, Arcavacata, 87036, Rende (CS), Italy*

[4]*NHAZCA S.r.l. & Department of Earth Sciences, Università di Roma "Sapienza", Via Cori snc, 00177, Roma, Italy*

Received: June 2, 2011. Accepted: March 1, 2012.

Numerical modelling is a major challenge in the prevention of hazards related to the occurrence of catastrophic phenomena. Cellular Automata methods were developed for modelling large scale (extended for kilometres) dangerous surface flows of different nature such as lava flows, pyroclastic flows, debris flows, rock avalanches, etc. This paper presents VALANCA, a first version of a Cellular Automata model, developed for the simulations of dense snow avalanches. VALANCA is largely based on the most advanced models developed for flow-like landslides, and adopts some innovations such as outflows characterized by the position of mass centre and explicit velocity. First simulations of well-documented snow avalanches occurred in the Davos region, Switzerland (i.e. the 2006 Rüchitobel and the 2006 Gotschnawang snow avalanches) show a satisfying agreement concerning the avalanche path, snow cover erosion depth, deposit thickness and areal distribution. Furthermore, preliminary simulations of the Gotschnawang snow-avalanche, by considering the presence of mitigation structures, were performed.

Keywords: Cellular automata, numerical modelling, computer simulation, snow avalanche, natural hazard, risk mitigation

* Corresponding author: E-mail: avoliomv@unical.it

1 INTRODUCTION

Snow avalanches are rapid gravity-driven movements of snow masses down mountain slopes. They may be included in the category of granular flows together with mudflows, debris flows, pyroclastic flows and rock avalanches. In fact, there is experimental evidence for snow avalanches exhibiting all the flow regimes identified in granular flows, from the quasi-static to the collisional, grain inertia and macroviscous regimes [1]. Moreover, the role of the interstitial fluid (air in most cases, an air/water mixture in slush avalanches) plays a decisive role in the transition between the quasi-static and collisional regimes on the one side, and the grain-inertia and macroviscous regimes on the other.

Dense avalanches have a high density core (100–500 kg/m^3) [2] at the bottom with particle sizes ranging from 1 mm to 1 m, typical flow depths between 0.5 and 5 m and velocities in the range 5–40 m/s [2]. They are a manifestation of the quasi-static and collisional regimes. On the other extreme, powder snow avalanches are dilute flows of small snow particles (< 1 mm) suspended in the air by intense turbulence. Here, the density is much lower than in dense avalanches (typically 1–10 kg/m^3), but the flow depth (10–100 m) and average velocity (30–100 m/s) are much larger [2]. In recent years, the important role of the fluidized regime, intermediate between these two end members, has been recognized (e.g., cf. [1–4]). Typical densities and flow velocities are 10–100 kg/m^3 and 30–70 m/s [2], respectively.

The urgent and increasing need for protection of settlements and traffic routes from snow avalanches has led to several approaches for modelling avalanches over the last 90 years [7]; nevertheless, the problem is still far from being completely resolved. Harbitz [7] gave a comprehensive overview of computational models for snow avalanches up to the end of the 20th century.

In order to put our proposed approach into context, we outline the statistical and fluid-mechanics approaches in the following.

Statistical approaches are based on comparison with historical avalanche data. The two main models are the α-β model [5] and the runout ratio model [6]. Both are based on the correlation existing between the runout distance and a set of topographic parameters describing the avalanche path. They assume that the longitudinal profile of the avalanche path governs avalanche dynamics.

The main shortcomings of statistical models are the lack of dynamical information (flow height, velocity, pressure) that is needed when designing protection measures and the difficulty of accounting for the specific properties of a given avalanche path (e.g., terrain roughness, channelization, snow drift) in an objective way. On the other hand, dynamical models offer a solution to both problems, but it has proved surprisingly difficult to develop

a reliable model because many different processes occur simultaneously and influence the motion of an avalanche.

There is a wide variety of fluid mechanics-based models; they differ in complexity and also with regard to the type of avalanche they describe [7]. Dense snow avalanches can be described by mass-point models (e.g. [8–11]) or continuum models based on the Navier-Stokes or Saint-Venant equations, with a constitutive equation appropriate for flowing snow. In the case of powder snow avalanches and slush flows, it may be necessary to use the binary mixture theory to suitably describe the dynamics of particles and interstitial fluid [12]. Models of the Saint-Venant type exploit the fact that snow avalanches (and in particular dense avalanches) are shallow flows by integrating the balance equations of mass and momentum (and energy) over the direction perpendicular to the ground (cf. [7, 13, 14] for more details and references to the original works).

A different approach, based on the Cellular Automata (CA) computational paradigm, was adopted by Barpi *et al.* [15], with the development of the model ASCA for the simulation of snow avalanches. Simulations of avalanches performed with ASCA, that occurred in Susa Valley (Western Italian Alps), were able to reproduce the correct three-dimensional avalanche path and the order of magnitude of the avalanche deposit. Likewise, Kronholm *et al.* [16] used a CA based model to show how the spatial structure of shear strength may be critically important for avalanche fracture propagation.

It is worth mentioning that CA models have been widely used to study the dynamics of sand piles, introducing "ad hoc" versions, e.g., Sand Automata [17, 18]. Sand Pile Models capture some important features (e.g., self organised criticality) of many natural complex phenomena, involving granular flows such as snow avalanches. Such models can investigate important natural hazards [19] with applications regarding mainly analyses in the time and frequency domain. Such models involve a probabilistic approach, that cannot be easily applied for simulating real macroscopic events with run-up effects, unlike ASCA and VALANCA models, that are strictly deterministic.

The next section introduces the methodological approach that was adopted in this work. Section 3 defines the model VALANCA, while the simulation results of two 2006 snow avalanches occurred in Davos region (Rüchitobel and Gotschnawang), Switzerland, are shown in section 4. The last section reports simulations, related to Gotschnawang area, for evaluating works for risk mitigation.

2 MODELLING SURFACE FLOW BY CELLULAR AUTOMATA

Cellular Automata (CA), a paradigm of parallel computing [20], are good candidates for modelling and simulating complex dynamical systems, whose evolution depends mainly on the local interactions of their constituent parts.

Very complex behaviours emerge by relatively simple local rules. Nevertheless, CA may represent sometime an alternative approach to differential equations for complex phenomena [20].

A Cellular Automaton evolves in a discrete space-time. Space is partitioned in cells of uniform size, and a state (from a finite set) is attributed to the cell; each cell embeds an identical computing unit, a Finite Automaton (FA), that changes the cell state according to the states of the neighbour cells, where the neighbourhood conditions are determined by a pattern invariant in time and space [20].

Natural phenomena are ordinarily modelled by three-dimensions CA with the cell corresponding to a volume of the real space. When several properties of the cell volume are determinant for the CA evolution, they are necessarily described by a large amount of states. These states may be formally represented by means of sub-states, where each sub-state specifies a property of the cells (e.g. temperature) and involve a complex transition function. This is an extension of classical CA [21], that was developed in order to model many complex macroscopic fluid-dynamical phenomena which seem difficult to be modelled in other CA frames (e.g. the lattice Boltzmann method [22]).

In the case of surface flows, quantities concerning the third dimension, i.e. the height, may be easily included among the CA sub-states (e.g. the altitude), thus allowing two dimensional models, yet working effectively in three dimensions. Furthermore, an algorithm for the minimisation of the differences in height [21, 23] was devised in this context in order to determine the outflows from a cell toward neighbourhood cells, thus giving rise to several models for macroscopic phenomena, such as lava flows [24], debris/mud flows [25] and rain soil erosion [26].

An explicit velocity solution is also adopted: moving flows toward the neighbouring cells are individuated by the sub-states mass, velocity and mass centre co-ordinates. The resulting new mass, mass centre and velocity are computed by composition of all the inflows from the neighbours and the residual quantities inside the cell [23, 25, 27, 28].

This paper illustrates VALANCA (the Sicilian word for avalanche and acronym for "Versatile model of Avalanche propagation by LAws and Norms of Cellular Automata"), a new model for the simulation of snow avalanches. VALANCA profits from studies of Barpi *et al.* [15], but includes new features [23] of SCIDDICA-SS2 ([25, 28]), the most advanced model of the SCIDDICA family [29] for flow-like landslides. Some differences, with respect to the ASCA model by Barpi *et al.*, are presented in Section 3.3.

3 THE MODEL VALANCA

The model VALANCA is based on the semi-empirical "equivalent fluid" approach [30]. By this approach, the dynamics of heterogeneous snow flow

is assumed to behave as a homogeneous flow usually integrated on depth. The constitutive features of the equivalent fluid, that are expressed by some VALANCA parameters, cannot be measured in laboratory, but are determined by back analyses of real cases.

Furthermore, the model is based on the following assumptions:

- the features of snow cover are considered as homogeneous;
- vertical layers of different density are not considered, but an average value of density is assumed;
- only dense snow avalanches are simulated.

The model is a two-dimensional CA with hexagonal cells, the state of cell is specified by sub-states, the transition function is constituted by local "elementary" processes, (specified better in the following) applied sequentially.

In formal terms, the model is defined as:

$$\text{VALANCA} = \langle R, X, S, P, \tau \rangle$$

where:

$R = \{(x, y) | x, y \in Z, -l_x \leq x \leq l_x, -l_y \leq y \leq l_y\}$ specifies part of a hexagonal tessellation by a finite set of regular hexagonal cells, where Z is the set of the integer numbers, each cell is identified by a couple of integer indexes (Figure 1), l_x and l_y are the extreme values of indexes. Each cell corresponds to a portion of real surface (a trivial metric may be introduced according to a CA parameter apothem, later specified, and neglecting the

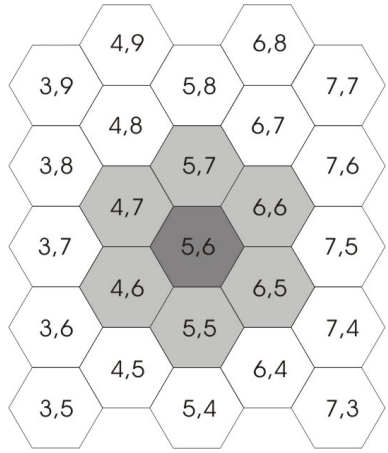

FIGURE 1
A piece of cellular space with co-ordinates of cells; the neighbourhood of cell (5, 6) is evidenced.

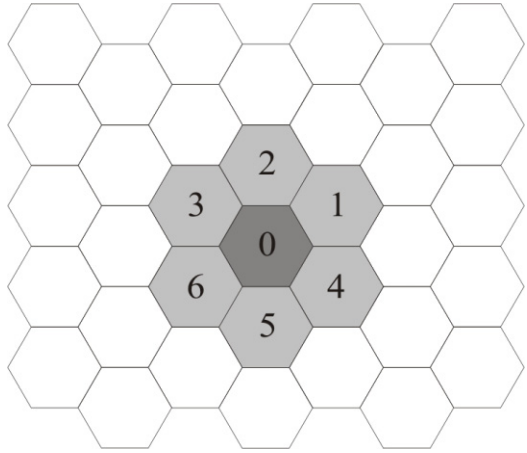

FIGURE 2
Example of neighbourhood for a generic cell in the cellular space (hexagonal tessellation).

altitude); of course R must cover the entire region, where the phenomenon evolves.

$X \equiv \{(0,0),(0,1),(0,-1),(1,0),(-1,0),(1,1),(-1,-1)\}$ identifies the geometrical pattern of cells, which influence any state change of the central cell (Figure 1 and Figure 2): the central cell itself with index 0 and the six adjacent cells with indexes $1,\ldots,6$; note that the sum of indexes of two opposite adjacent cells is always 7 by convention. This helps to write formulas in a not muddled way; for instance, the inflow from the *i-th* cell of the neighbourhood toward the central cell (opposite direction $7-i$) is specified as $E_{7-i}[i]$;

$S = S_A \times S_D \times S_{TH} \times S_X \times S_Y \times S_{KH} \times S_E^6 \times S_{XE}^6 \times S_{YE}^6 \times S_{KHE}^6 \times S_I^6 \times S_{XI}^6 \times S_{KHI}^6$ is the finite set of states of the finite automaton, embedded in the cell; it is equal to the Cartesian product of the sets of the considered sub-states:

- S_A (m) is the cell altitude;
- S_D (m) is the snow cover depth, that could change into avalanche mass by erosion (Figure 3);
- S_{TH} (m) is the average thickness of avalanche mass inside the cell (Figure 3), S_X and S_Y (m) are the co-ordinates of the mass centre with reference to the cell centre;
- S_{KH} (m) is the kinetic head of avalanche mass inside the cell;
- S_E (m) is the part of avalanche mass, the so called "external flow", (normalised to a thickness) that enters the adjacent cell from central cell, S_{XE} and S_{YE} (m), are the co-ordinates of the external flow mass

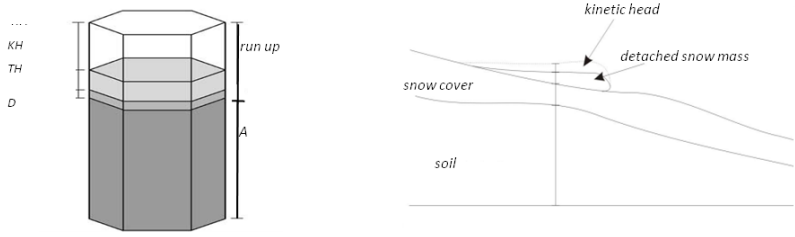

FIGURE 3
Left: three-dimension visualization of the sub-states *A*, *D*, *TH* and *KH* for a hexagonal cell. Right: an ideal vertical section of a snow flow

centre with reference to the adjacent cell centre, S_{KHE} (m) is the kinetic head of avalanche mass flow. There are six components (one for each adjacent cell) for the sub-states S_E , S_{XE} , S_{YE} , S_{KHE};

- S_I (m) is the part of avalanche mass towards the adjacent cell, the so called "internal flow", (normalised to a thickness) that remains inside the central cell, S_{XI} and S_{YI} (m) are the co-ordinates of the internal flow mass centre with reference to the central cell centre, S_{KHI} (m) is the kinetic head of avalanche mass flow. There are six components (one for each adjacent cell) for the sub-states S_I , S_{XI} , S_{YI} , S_{KHI}.

$P = \{p_a, p_t, p_{fc}, p_{td}, p_{ed}, p_{mt}, p_{pe}, p_\rho\}$ is the set of the global physical and empirical parameters, which account for the general frame of the model and the physical characteristics of the phenomenon; the next section provides a better explication of the elements of the following set:

- p_a (m) is the cell apothem;
- p_t (s) is the temporal correspondence of a CA step;
- p_{fc} (dimensionless) is the friction coefficient for avalanche outflows;
- p_{td}, p_{ed} (dimensionless) are parameters for energy dissipation by turbulence and erosion;
- p_{mt} (m) is the activation thresholds of the snow mobilisation;
- p_{pe} (dimensionless) is the progressive erosion parameters;
- p_ϱ (kg/m^3) is the snow density.

$\tau : S^7 \to S$ is the deterministic state transition function for the cells in R. The basic elements of the transition function will be sketched in the next section.

It is worth to note that when the set of sub-states (e.g., corresponding to a physical quantity) can range in a continuous interval between two values, a

finite, but sufficient number of significant digits are utilised. In this case, the set of permitted values is large but finite, according to the CA definition, and the required precision can be reached.

In the following, variables concerning sub-states and parameters are indicated by their abbreviation subscript (e.g. TH and t refer to S_{TH} and p_t). When sub-states need the specification of the neighbourhood cell, it is indicated between square brackets (e.g. $TH[2]$ refers to S_{TH} of the neighbour with index 2). Multi-components sub-states differ by a subscript index (e.g. KHE_2 refers to the second component of S^6_{KHE}). nQ and ΔQ respectively indicate the new value and variation of the sub-state S_Q.

At the beginning of the simulation, we specify the states of the cells in R, defining the initial CA configuration. The initial values of the sub-states are accordingly initialised. In particular, A assumes the morphology values; D assumes initial values corresponding to the maximum depth of the snow mantle cover except for the detachment area, where the thickness of the detached avalanche mass is subtracted from the snowpack depth; TH is zero everywhere except for the detachment area, where the thickness of detached avalanche mass inside the cell is specified; all values related to the remaining sub-states are zero everywhere.

At each next step, the function τ is applied to all cells in R, so that the configuration changes in time and the evolution of the CA is obtained.

3.1 The VALANCA Transition Function

The state transition function τ must account for all the processes (physical, chemical, etc.), which are assumed to be relevant to the system evolution, specified in terms of state changes in the CA space. As well as the state of the cell can be decomposed in sub-states, the transition function τ may be split into "elementary" processes, that are applied sequentially according to a defined order. Each elementary process involves the update of the states of the cells. The application of all the elementary processes constitutes a CA step.

Four local processes are here considered for VALANCA:

- snow cover, kinetic head and avalanche thickness variation by snow cover mobilisation;
- kinetic head variation by turbulence dissipation;
- avalanche outflows (height, mass centre co-ordinates, kinetic head) determination and their shift deduced by the motion equations;
- composition of avalanche mass inside the cell (remaining avalanche plus inflows) and determination of new thickness, mass centre coordinates and kinetic head.

Let us here recall the simple physics formula related to energy computation, which are derived from the model discretization. Consider a “column" of mass m (with constant density ρ), with base B, thickness h at altitude z, previously explained, which moves at velocity v (Figure 3). If E_u and E_k represent the potential and the kinetic energy, respectively, the total energy of the column, E_T, is given by the following expression:

$$E_T = E_u + E_k = \rho g B \int_z^{z+h} z dz + \frac{1}{2}\rho B h v^2 = \rho g B h \left(\frac{h}{2} + z\right) + \frac{1}{2}\rho B h v^2 \tag{1}$$

where g is gravity acceleration. In hydrodynamics ([31,32]) the kinetic head, h_k, is defined as:

$$h_k = \frac{v^2}{2g} \tag{2}$$

which describes a fictitious height representing the kinetic energy per unit of weight of the cell material given by Equation 2.

The previous “singular" considerations are useful, as VALANCA generally handles “quantities" in terms of heights (e.g. volume, velocity, energy). Accordingly, the above formula of total energy can be rewritten as:

$$E_T = \rho g B h \left(\frac{1}{2}h + z + h_k\right) \tag{3}$$

Consequently, h_k can be directly computed from the total energy, E, as:

$$h_k = \frac{E_T}{\rho g B h} - z - \frac{1}{2}h \tag{4}$$

and, accordingly:

$$E_k = \frac{1}{2}m v^2 = m g h_k = B \rho g h h_k \tag{5}$$

where B, in this context, indicates the area of the hexagon with apothem a, $B = 2\sqrt{3}a^2$.

Recall that the total energy, E_T, the kinetic energy, E_k, the thickness, h and the kinetic head, h_k, in the following paragraphs will be marked with the words *TE*, *KIN*, *TH* and *KH*, respectively.

In the following, a sketch of the local elementary processes will be given, which is sufficient to capture the mechanisms of the transition function.

Mobilisation Effects
When the kinetic head value overcomes an opportune threshold, $KH > mt$, depending on the snow cover features, a mobilisation of the snow cover occurs, which is proportional to the quantity overcoming the threshold:

$$pe\,(KH - mt) = \Delta TH = -\Delta D$$

(the snow cover depth diminishes as the avalanche thickness increases), the kinetic head loss is: $-\Delta KH = ed\,(KH - mt)$. This implies a loss of kinetic energy according to formula 5; thus, the new value of kinetic energy is:

$$KIN = 2\sqrt{3}a^2\rho g\,(KH + \Delta KH)\,TH \tag{6}$$

The mixing of the eroded snow cover with the earlier avalanche mass involves that the earlier kinetic energy of avalanche mass becomes the kinetic energy of all the avalanche mass, because kinetic energy of the eroded snow cover was null: it implicates trivially a further kinetic head reduction.

$$KIN = 2\sqrt{3}a^2\rho g\,(KH + \Delta KH)\,TH = 2\sqrt{3}a^2\rho g\,(TH + \Delta TH)\,nKH \tag{7}$$

then

$$nKH = \frac{TH\,(KH - ed\,(KH - mt))}{(TH + \Delta TH)} \tag{8}$$

Turbulence Effect
The effect of the turbulence is modelled by a proportional kinetic head loss at each VALANCA step:

$$-\Delta KH = tdKH \tag{9}$$

This formula involves that a velocity limit is imposed "de facto". A generic case with a maximum value of slope may be always transformed in the worst case of an endless channel with constant maximum slope value. In this case, an asymptotic value of kinetic head is implied by infinite formula applications and, therefore, a velocity limit is deduced. Note that rotational effects are not considered explicitly, because the model accounts only for simple displacements of mass between couples of cells (discussed next), but rotational effects involve energy reduction, that is modelled as turbulence effect.

Avalanche Mass Outflows
Outflows computation is performed in two steps: determination of the outflows minimising the "height" differences in the neighbourhood ([21, 23]) and determination of the shift of the outflows.

The minimisation algorithm defines a central cell quantity d to be distributed, $d = \sum_{i=0}^{n} f[i]$, where $f[i]$ is the flow towards the cell i ($f[0]$ is the part of d, which remains in the central cell); $h[i]$, $0 \leq i \leq 6$ are the quantities that specify the "height" of the cells in the neighbourhood, to be minimised by contribution of flows: more precisely, the algorithm minimises the expression [23]:

$$\sum_{\{(i,j)0 \leq i \leq j \leq 6\}} |(h[i] + f[i]) - (h[i] + f[i])| \tag{10}$$

Avalanches are rapid flows and imply a run up effect, depending on the kinetic head associated to debris flow. As a consequence, the height minimisation algorithm [21] is applied, considering for the central cell $h[0] = A[0] + KH[0] + D[0]$ and $d = TH[0]$; $h[i] = A[i] + TH[i] + D[i]$, $1 \leq i \leq 6$, for the adjacent cells; note that $KH[0]$ accounts for the ability of climbing a slope for the flowing avalanche. The minimisation algorithm determines the flows $f[i]$, $0 \leq i \leq 6$ toward the neighbouring cells ($f[0]$ is the part of d which is not distributed); such flows minimise the expression 10.

The mass centre co-ordinates x and y of moving quantities are the same of all the avalanche mass inside the cell and the form is ideally a "cylinder" tangent the next edge of the hexagonal cell (Figure 4). The height difference $h[0] + d - h[i]$ determines an ideal slope $\theta[i]$ between the two cells 0 and i; a preliminary test is executed in order to account for friction effects, which prevent avalanche outflows, when $tan(\theta[i]) < fc$. An ideal length "l" is considered between the avalanche mass centre of central cell and the centre of the adjacent cell i including the slope $\theta[i]$, representing the maximum allowed path of the outflow.

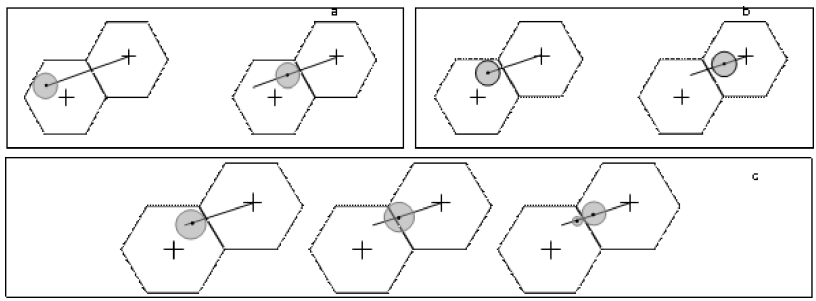

FIGURE 4
Determination of the outflow shift. (a) All the cylinder remains in the cell: the flow is only internal and contributes to change the new centre mass of the cell. (b) All the cylinder leaves the cell: the flow is only external. (c) Part of the cylinder crosses the cell: there are both internal and external flows.

The $f[i]$ shift "sh" is computed for avalanche outflows according to the following simple formula, which averages the movement of all the mass as the mass centre movement of a body on a constant slope with a constant friction coefficient:

$$sh = v \cdot t + g\,(sin\theta - fc \cdot cos\theta)\,\frac{t^2}{2} \tag{11}$$

with g being the gravity acceleration and the initial velocity $v = \sqrt{2gKH}$.

The motion involves three possibilities (Figure 4): (1) only internal flow: the shifted cylinder is completely internal to the central cell, (Figure 4.a); (2) only external flow: all the shifted cylinder is external to the central cell inside the adjacent cell, (Figure 4.b); (3) the shifted cylinder is partially internal to the central cell and partially external to the central cell, (Figure 4.c). In this case, the flow is divided between the central and the adjacent cell, forming two cylinders with mass centres corresponding to the mass centres of the internal flow and the external flow.

The kinetic head variation is computed according to the new position of internal and external flows, while the energy dissipation was considered as a turbulence effect in the previous elementary process.

Note that *fc* and *td* concur in different ways to the deposition of the material: *fc* involves a slope threshold θ that blocks the snow movement when the kinetic energy is null, otherwise there is a deceleration; *td* ensures for a constant slope larger than θ angle a limit in the acquisition of the kinetic head *KH*, therefore of kinetic energy *KIN*. Stopping occurs only if the slope is below the θ angle and is dependent in time on the cumulated kinetic energy *KIN*.

The previous approach resounds the studies of Voellmy [9], who used a first simple empirical formula, treating an avalanche as a sliding block of snow moving with a drag force that is proportional to the square of the speed of its flow and with a frictional effect on the sliding surface. VALANCA describes the snow avalanche as composed of many flows between couples of cells. An outflow between two cells in VALANCA consists of a sort of sliding cylindrical block, with an initial velocity in a slope with angle θ. VALANCA computes (equation 11) the block shift, accounting only for an energy loss, determined by friction coefficient; furthermore VALANCA (equation 6) computes the turbulence loss of energy, proportionally to the square of the speed, since the kinetic head is proportional to the square of the velocity (equation 2).

Flows Composition

When avalanche mass outflows are computed, the new situation involves that external flows leave the cell, internal flows remain in the cell with different

co-ordinates and eventually the presence of inflows (trivially derived by the values of external flows of neighbour cells). The new value of TH is given by considering the balance of inflows and outflows with the remaining snow mass in the cell.

$$nTH\,[0] = TH\,[0] + \sum_{i=1}^{6} I_{7-i}\,[i] - \sum_{i=1}^{6} E_i\,[0] + \sum_{i=1}^{6} E_{7-i}\,[i] \tag{12}$$

A further kinetic energy reduction is considered by loss of flows, while an increase is given by inflows. In order to perform this operation, the total energy of the cell, TE, and the total energy of each external outflow i, TE_i, are computed according to equation 3. By applying equations 4 and 5, we obtain:

$$nKIN = \rho g 2\sqrt{3}a^2 nTH \left(\frac{TE - \sum_{i=1}^{6} TE_i[0] + \sum_{i=1}^{6} TE_{7-i}[i]}{\rho g 2\sqrt{3} nTH} - A - \frac{1}{2} nTH \right) \tag{13}$$

therefore, consequently with 3.1.5, the new value of the kinetic head is deduced from the computed kinetic energy as follows:

$$nKH = \frac{nKIN}{\rho g 2\sqrt{3}a^2 nTH} \tag{14}$$

The co-ordinates determination is calculated as the average weight of X and Y by considering the remaining snow mass in the central cell, the internal flows and the inflows

$$nX[0] = \frac{(\Gamma \times X[0] + \sum_{i=1}^{6} E_{7-i}[i] \times XE_{7-i}[i] + \sum_{i=1}^{6} I_i[0] \times XI_i[0]}{nTH[0]} \tag{15}$$

$$nY[0] = \frac{(\Gamma \times Y[0] + \sum_{i=1}^{6} E_{7-i}[i] \times YE_{7-i}[i] + \sum_{i=1}^{6} I_i[0] \times YI_i[0]}{nTH[0]} \tag{16}$$

where

$$\Gamma = TH[0] - \sum_{i=1}^{6} E_i[0] - \sum_{i=1}^{6} I_i\,[0]$$

3.2 An implementation for VALANCA

VALANCA was implemented in ANSI C++ in order to obtain a well-structured, efficient and extensible source code. The main steps of VALANCA, are shown in Figure 5.

```
begin
      Read input data;
      Assign the initial state of cells;
      repeat
            Increment time step;
            for all cells in the matrix R do
                  begin
                   Determine the global indices of neighbouring cells;
                   Calculate outflows (by means of the Minimisation Algorithm);
                   Determine outflows shift deduced by the motion equations;
                   Calculate effective flow (external and internal flow);
                   Compose flows and determine the new thickness, mass centre
                        coordinates and kinetic head;
                   Verify mobilisation of the snow cover;
                   Calculate kinetic energy reduction for turbulence;
                   Update the total energy;
                  end
      until flow velocity is null in all cells containing snow
end
```

FIGURE 5
Main steps of VALANCA.

The new value of *TH* is given by considering the balance of inflows and outflows with the remaining snow mass in the cell. The program is characterised by a command line interface that allows the user to interactively control all input/output and simulation, and to visualize the simulation in real time. Through the viewer module, it is also possible to observe the DTM over which the phenomenon evolves and perform both a visual and quantitative comparison with the real case in terms of the evaluation function f_a, later defined.

3.3 Some Relevant Differences Between VALANCA and ASCA

ASCA [15] is a CA model for the simulation of snow avalanches, with many analogies with VALANCA. As a matter of fact, both are two-dimensions models based on hexagonal cells and are ruled by the same flow distribution algorithm [16]. The models distinctions are synthesized in the following points.

ASCA shares with many CA models ([25, 27, 28]) an approach that does not permit to make velocity explicit: a fluid amount moves from a cell to another one in a CA step, which corresponds usually to a constant time. This implies a constant local "velocity" in the CA context of discrete space/time, even if a kind of flow velocity emerges by averaging on the space (i.e. considering clusters of cells) or by averaging on the time (e.g. considering the average velocity of the advancing flow front in a sequence of CA steps). Conversely, VALANCA inherits characteristics of the latest releases of SCIDDICA [25, 28], that introduce coordinates of mass centre of flows and computes their shift. In this case, velocity is indeed locally explicit (see Section

3.1, Avanche Mass Outflows). The introduction of mass centres has introduced improvements in simulations in terms of fitness, despite an inevitable slight worsening in execution times over the considered simulations.

Note that energy losses related to the kinetic head (see Section 3.1, Turbulence Effect) are handled in ASCA according different formulae, deduced by PDE type approaches [33]. In ASCA, the considered test-case snow avalanche was extremely rapid and thus characterised by relevant run-up effects, whose physical meaning is the minimum height of an obstacle needed to stop the motion of a mass with thickness moving at a certain velocity. Here, the run-up is determined by the thickness of the snow plus a fictitious height, which corresponds to the kinetic head and represents (Figure 3) in the minimization process, a conservative quantity which has to be distributed among the neighbouring cells in order to reach the conditions of maximum stability. At the contrary, in the VALANCA model, the run-up effect for fast moving snow avalanches is expressed in a different manner. Here, the kinetic head is not considered as a whole with the snow (i.e., it is not considered as a mobile part during the minimization process) but computed separately from it in order to explicitly consider the physical characteristics related to energy loss and avalanche velocity related to the kinetic head itself (again in Section 3.1, Turbulence Effect).

4 SNOW AVALANCHES SIMULATION BY VALANCA

A first validation and calibration of the parameters of VALANCA has been performed by back-analysis, simulating two snow avalanches occurred in 2006 in Davos (Switzerland) and well described in [34]. Furthermore, test avalanches were selected since they were well known in terms of areal path, thickness, deposit, velocity during the propagation, etc.

During the winter season, the Davos area is frequently affected by a great number of avalanche events. The first considered event occurred on January 20, 2006, when a dry-snow avalanche was released artificially from the Gotschnawang slope in the Parsenn ski area (municipality of Klosters, Eastern Switzerland) to protect the intermediate station of the Gotschna telepher. The avalanche covered an area of 230 ha and was 750 m long (projected length) with a vertical drop of 460 m, corresponding to a runout angle of 31.5°, which is a fairly large value for a dry-snow avalanche of this size. The site is an open but very hummocky slope with a straight track. The release area was 400 m wide, and the release depth estimated at 40 cm (Figure 6).

The avalanche developed a fluidized layer whose deposits are visible both on the right-hand side and in the frontal part. The fluidized layer ran up to 50 m farther than the dense part and its mass was estimated at 100 tons, compared to 3000 tons for the dense part.

FIGURE 6
Gotschnawang avalanche. Outline of the 2006-01-20 Gotschnawang avalanche (Davos, Switzerland). The extent of the fracture line is indicated by the dotted line.

The second event occurred on January 18, 2006, when a dry-snow avalanche involved the Rüchitobel gully, Dischma Valley (Davos, Eastern Switzerland) (Figure 7). The avalanche covered an area of 10 ha and was 1167 m long (projected length) with a vertical drop of 630 m. The irregularly shaped release area was 195–290 m wide, with an estimated average release depth of 90 cm. For about 650 m (projected length), the flow was channelled in a winding gully whose bottom is around 10–15 m wide and was covered by 0.5–1.5 m deep deposits from this avalanche, stacked over those from earlier ones, while the new snow was eroded completely.

FIGURE 7
Rüchitobel avalanche. Outline of the 2006-01-18 Rüchitobel avalanche (Davos, Switzerland). The extent of the fracture line is indicated by the top dotted line.

On the upper parts of the gully banks and to the sides, the traces of fluidised layer were clearly observable to a height of 10–15 m above the gully bottom in which the snow was completely eroded away, without any deposits. In the most pronounced bend, the angle between the top flow marks of the fluidised part on either side and the tilt of the surface of the dense deposit indicated maximum flow velocities 28–38 m/s and 10–20 m/s, respectively. On the left-hand side and also at the distal end of the runout area, the deposit showed the characteristic features expected from fluidised flow. The mass of the dense deposit was estimated at 4000 tons while the fluidised one was only 40–50 tons (1% of the avalanche mass).

The first analysed event (Gotschnawang) is quite challenging from a modelling point of view since it occurred in an open slope, while the second one (Rüchitobel) represents an interesting example of channelled snow avalanche. Detailed data of snow avalanches were available: among them, the release area and volume, avalanche path, the spatial distribution and local thickness of the final deposit, the snow density in the snow cover and in the deposit. Furthermore, in a few cases the propagation velocities could be estimated at specific points. Snow cover entrainment occurs in both cases, and also traces of fluidized flow were detected. However, the model simulates, as a first attempt, only dense flows.

The same set of parameters (Table 1) has permitted to reproduce the two considered snow avalanches with a great level of accuracy. Specifically, the global parameters of the model are: the apothem, a, of the hexagon; the time step duration, t, i.e., the time interval between successive upgrades of the system state and the density, ϱ, of the avalanche material. This latter is assumed to be constant throughout the simulation [33, 35–37]. Although the physical sense of some other parameters (i.e., the friction coefficient, fc; energy dissipation parameters by turbulence, td, and erosion, ed) is well defined,

Characteristic	**Gotschnawang**	**Rüchitobel**
Cell apothem a (m)	2.5	2.5
CA matrix size (cells)	283×199	283×219
Time step t (s)	0.16	0.16
Friction coefficient fc	0.3	0.3
Energy loss by turbulence td	0.145	0.145
Energy loss by erosion ed	0.00001	0.00001
Thresholds of mobilisation mt (m)	7	7
Progressive erosion pe	0.155	0.155
Snow density ϱ (kg/m^3)	150	150
Volume of eroded snow in the simulation	21619	11424

TABLE 1
Set of adopted global parameters for VALANCA in the carried out simulations.

their value in the present paper are rather considered as the best parameters obtained on the basis of back-analyses of the observations of real events. The remaining parameters (i.e., the activation threshold of the snow mobilisation, mt, and the progressive erosion, pe) are of empirical nature.

First calibrations were performed as usual by a preliminary trial and error method; results were good enough that it was not necessary to use other accustomed automatic time consuming calibration techniques [38] (e.g. by means of Genetic Algorithms).

Simulation times depend on the number of active cells processed for each step and on the number of steps, necessary to complete the phenomenon: for instance, 10000 cells processing in a CA step last approximately 0.5 s on a 2.4 GHz dual-core PC. The Gotschnawang simulation takes about three minutes with a 199×283 CA matrix excluding interactive graphical output. Several simulations were performed in order to calibrate the parameters and best results are described in the following.

A first comparison between the real events and the simulated ones is performed by a fitness function, f_a [38], concerning areas and computed by the following formula: $\sqrt{\frac{R \cap S}{R \cup S}}$ where R, in this case, is the set of cells affected by the avalanche in the real event and S the set of cells affected by the avalanche in the simulation. Note that f_a returns a normalised value between 0 (complete failure) and 1 (perfect simulation).

Both avalanches were back-analysed by the VALANCA model by using a 5 m cells DTM by taking into account the release area, the portion of the slope covered by the snow mass and the erosion during the propagation.

In the Gotschnawang simulation (Figure 8) a surprising areal agreement between the real event and the simulation was achieved corresponding to a fitness $f_a = 0.92$.

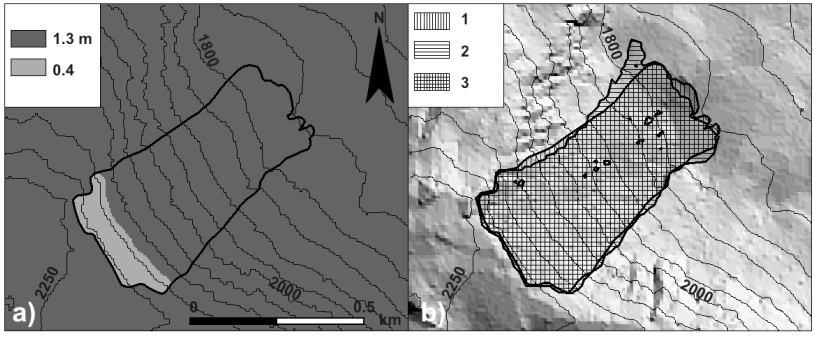

FIGURE 8
The 2006 avalanche in Gotschnawang: (a) snow cover with detachment area and real event, (b) post-event DEM, superposition (3) of real (1) and simulated (2) event.

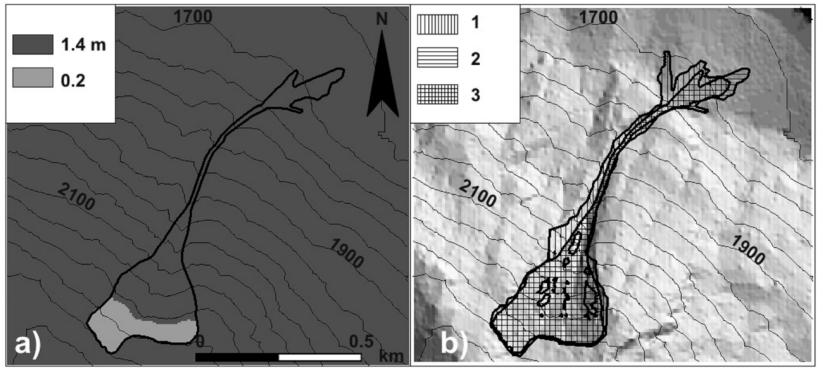

FIGURE 9
The 2006 avalanche in Rüchitobel: (a) snow cover with detachment area and real event, (b) post-event DEM, superposition (3) of real (1) and simulated (2) event.

The Rüchitobel simulation (Figure 9) best results corresponded to a value of f_a close to 0.81, which is considered a satisfying preliminary result if the complex geometry of the avalanche path is taken into account.

A further analysis of simulation results show how extreme offshoots of the avalanche spread in a fan-like manner, according to the morphology, while this effect is weaker for the real case. This implies that a more accurate management of momentum must be introduced in order to obtain more precise results.

5 MODELLING SNOW-AVALANCHE-STRUCTURES INTERACTION: VALANCA PROSPECTS FOR RISK MITIGATION

Forecasting dynamics of a snow avalanches could be a fundamental component for risk mitigation. Numerical simulation permits to determine the physical evolution of the phenomenon considering impact areas, related avalanche energy and other characteristics for the most probable and significant scenarios. Moreover, numerical simulations permit estimations of avalanche physical characteristics (i.e. flow depths, velocities, deposit heights) necessary for control structures planning.

Two different types of avalanche control structures are commonly distinguished: structures in the starting zone (i.e. permanent steel supporting structures and wood supporting structures) which prevent avalanche triggering and structures in the track and runout zones which reduce damaging effects of descending avalanches. In the track or run-out zones, deflecting structures

such as walls or dams, may change avalanche moving direction and deflect it from the object to be protected. In the runout zone, retarding structures (i.e. catching dams or retarding mounds) reduce avalanche speed and shorten the runout distance [39].

A very preliminary study was performed in order to assess the behaviour of VALANCA in presence of mitigations works (i.e. deflecting dam). Control structures planning is usually carried out on events with quite long return periods (i.e. 30-500 yrs in Switzerland), while the return period of the avalanche of this study is quite short (1-10 yrs). As a consequence, it must be said that for a realistic planning long-term avalanches are needed to be taken into account.

It is worth to note that the main point of these works is the complex interaction between snow (direction, density and so on) and the structures of the work (resistance, energy dissipation and so on). The introduction of different types of passive works in VALANCA involves new sub-states and new elementary processes for each type of mitigation work. In VALANCA, this application consists in a fixed alteration of altitude for a line of cells. In particular, a deflection dam, whose resistance is considered unlimited, is created corresponding to a trivial variation (increment) of the morphology which permits to correctly use the present version of VALANCA. Buildings are considered in the same way: the cell altitude is altered in relation to height (on average) of that part of building which "covers" the cell; even in this case, resistance is ideally considered infinite.

The same area concerning the 2006 Gotschnawang avalanche was selected in order to simulate some case studies, where the intermediate station of the Gotschnawang telepher could be considered. Due to its quite safe position, the telepher has been "relocated" in an more unsafe position (Figure 10), in order to test the behaviour of VALANCA simulated avalanche in case of a deflecting dam protecting the dislocated building.

Deflecting dams of different lengths and heights were considered with an angle of about 39° respect to the avalanche direction, about 13 meters far from the dislocated telepher station. Many simulations were performed with the same initial conditions of the 2006 Gotschnawang avalanche, except the presence of a dam and the building dislocation.

We selected four simulations (Figure 10) with different values of height and length of dams:

$\langle h\ 2m,\ l\ 165m\rangle$, $\langle h\ 4m,\ l\ 50m\rangle$, $\langle h\ 4m,\ l\ 110m\rangle$, $\langle h\ 4m,\ l\ 160m\rangle$, where h and l are the height and length of the dams, respectively.

A first simulation (Figure 10.a) shows that 2m in height is not sufficient for protecting the dislocated building, even if the length (165m) covers abundantly all the building extension in relation to the avalanche direction.

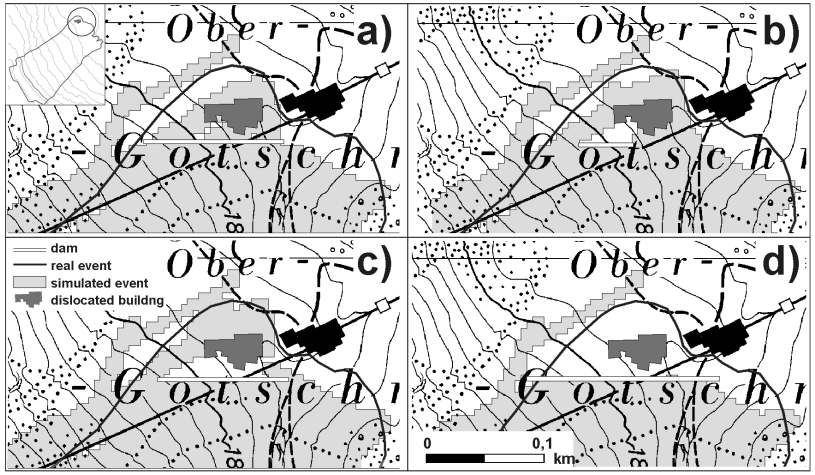

FIGURE 10
Effects of deflecting dams of different lengths and heights: (a) 2m height and 165m length, (b) 4m height and 50m length, (c) 4m height and 110m length, (d) 4m height and 160m length.

The remaining simulations (Figure 10 b, c, d) consider 4m height dams with different lengths, 50m, 110m and 160m respectively. In this case, the protection effect is not proportional to the length, where a threshold, around 150m, enlarges suddenly the safe area.

These simulations must be considered as a simple application which, however, allowed us to infer the capability of VALANCA in simulating the interaction between snow avalanches and mitigations structures.

Achieved results are considered promising by the authors. However, some improvements of the snow-structure module of VALANCA will be carried out, in order to make the model more physically based and reliable. In particular, as previously reported, control structure planning is based on reference parameters on long-term events, so further studies are needed. In addition, other improvements will be carried out on the modelling of the components of the simulated avalanche that in this case consists only in the dense part.

6 CONCLUSIONS

A CA model for simulating snow avalanche dynamics (VALANCA) has been developed and tested over real cases. Such a model represents an interesting improvement with respect to the ASCA model [15], since it allows to explicit compute velocity which is a key parameter for the estimation of snow avalanches' magnitude. Preliminary model validation and calibration

has been performed by back-analysing the Rüchitobel and Gotschnawang snow avalanches occurred in 2006 in Davos (Switzerland). Results, discussed in this paper, prove the ability of the model to simulate such a type of events in a satisfying way. The real path of the snow avalanche has been well simulated in both open and channelled slopes. However, in spite of the encouraging results, the model needs several improvements in order to be used for forecasting analyses of snow avalanches propagation. In particular, the main transition function improvements regard a better approximation in erosion and snow entrainment computation, besides a better numerical management of momentum and avalanche velocity.

The introduction of snow avalanche interaction with structures and man-made works represent a further important improvement of the VALANCA model with respect to already existing ones. Notwithstanding, the rough method used for a preliminary study of snow avalanche risk shows without doubt as enhanced versions of VALANCA could be usefully used in hazard and risk analyses for snow avalanches. With this objective, an improvement of the model VALANCA is planned together with its applications to other cases of different type of snow avalanches.

ACKNOWLEDGEMENTS

The authors wish to thank Dr. Dieter Issler for useful comments and suggestions in the first draft of the paper.

REFERENCES

[1] Issler, D., Gauer, P., Schaer, M., Keller, S. (1996). Staublawinenereignisse im Winter 1995: Seewis (GR), Adelboden (BE) und Col du Pillon (VD). SLF Internal Report 694. Eidg. Institut für Schnee- und Lawinenforschung, Davos, Switzerland.

[2] Issler, D., Errera, A., Priano, S., Gubler, H., Teufen., B., Krummenacher B. (2008). Inferences on flow mechanims from snow avalanche deposits. *Annals of Glaciology*, 49, 187–192.

[3] Schaerer, P.A., Salway, A.A. (1980). Seismic and impact-pressure monitoring of flowing avalanches. *J. Glaciol.*, 26 (94), 179–187.

[4] Issler, D., Gauer, P. (2008). Exploring the significance of the fluidised flow regime for avalanche hazard mapping. *Annals of Glaciology*, 49, 193–198.

[5] Lied K., Bakkehøi S. (1980). Empirical calculations of snow-avalanche run-out distance based on topographic parameters. *Journal of Glaciology*, vol. 26, Issue 94, pp. 165–177.

[6] McClung D.M., Lied K. (1987). Statistical and geometrical definition of snow avalanche runout. *Cold Regions Science and Technology*, vol. 13, Issue 2, 107–119.

[7] Harbitz, K. (1999). A survey of computational models for snow avalanche motion. Tech. Rep. Fourth European Framework Programme (ENV4-CT96-0258) Avalanche Mapping, Model Validation and Warning Systems.

[8] Perla, R.I., Cheng, T. T., McClung, D. M. (1980). A two parameter model of snow avalanche motion. *J. Glaciol.*, 26 (94), 197–202.

[9] Voellmy, A. (1955). über die Zerstörungskraft von Lawinen. Schweizerische Bauzeitung. 73 159–165, 212–217, 246–249, 280–285.

[10] Salm, B. (1968). On nonuniform, steady flow of avalanche snow. Procedings of the General Assembly of Berne, 1967 Snow and Ice. IAHS Publ. n° 79. International Association of Hydrological Sciences, Wallingford, Oxfordshire, UK. Pages 19–29.

[11] Salm, B., Bukard., Gubler, H. U. (1990). Berechung von Fliesslawinen. Eine Anleitung für Praktiker mit Beispielen. Mitteleilung del SLF n° 47. Istitut Federal Suisse pour l'Etude de la Neige et des Avalanches, CH-7260 Davos Dorf, Suisse.

[12] Eglit, M.E. (1998). Mathematical and physical modelling of powder snow avalanches in Russia. *Annals of Glaciology*, 26, 281–284.

[13] Pudasaini, S.P., Hutter, K. (2007). Avalanche Dynamics: Dynamics of Rapid Flows of Dense Granular Avalanches. Berlin, Germany, Springer.

[14] Ancey, C. (2001). Snow Avalanches. in Geomorphological Fluid Mechanics: Selected Topics in Geological and Geomorphological Fluid Mechanics, In Balmforth N.J, Provenzalle, A., (eds.), pp. 319–338, Springer-Verlag, New York.

[15] Barpi, F., Borri-Brunetto, M., Delli Veneri, L. (2007). Cellular-Automata Model for Dense-Snow Avalanches. *Journal of Cold Regions Engineering*, 21 (4) 121–140.

[16] Kronholm, K., and Birkeland, K. W. (2005). Integrating spatial patterns into a snow avalanche Cellular Automata model, Geophysical. Research Letters, 32, L19504, 4 pp., doi:10.1029/2005GL024373.

[17] Goles Ch., E., Kiwi, M.A., (1993). Games on Line Graphs and Sand Piles. *Theor. Comput. Sci.*, 115, 321–349.

[18] Dennunzio, A., Guillon, P., Masson B., (2009). Sand Automata as cellular automata. *Theor. Comput. Sci.*, 410, 3962–3974.

[19] Bak, P., (1997). How Nature Works. The Science of SOC, Oxford University Press.

[20] Wolfram, S., (2002). A new kind of science. Wolfram Media, Inc, Champaign.

[21] Di Gregorio, S., Serra, R. (1999). An empirical method for modelling and simulating some complex macroscopic phenomena by Cellular Automata. *FGCS*, 16, 259–271.

[22] Succi, S., Benzi, R., Higuera, F. (1991). The lattice Boltzmann equation: a new tool for computational fluid dynamics. *Physica*, 47 D (1991) 219–230.

[23] Avolio, M.V. (2004). Esplicitazione della velocità per la modellizzazione e simulazione di flussi di superficie macroscopici con automi cellulari ed applicazioni alle colate di lava di tipo etneo. PhD. Thesis (in Italian). *Dept. of Mathematics*, University of Calabria.

[24] Avolio, M.V., Crisci, G.M., Di Gregorio, S., Rongo, R., Spataro W., Trunfio, G.A., (2006). SCIARA $\gamma 2$: an improved Cellular Automata model for Lava Flows and Applications to the 2002 Etnean crisis. *Computers & Geosciences*, Vol. 32 pp. 897–911, 2006.

[25] Avolio, M.V., Lupiano, V., Mazzanti, P., Di Gregorio, S. (2008). Modelling combined subaerial-subaqueous flow-like landslides by Cellular Automata. In H. Umeo *et al.* (eds), ACRI 2008, LNCS, 5191, pp. 329–336. Springer, Heidelberg.

[26] D'Ambrosio, D., Di Gregorio, S., Gabriele, S., Gaudio, R. (2001). A Cellular Automata Model for Soil Erosion by Water. *Phys. Chem. Earth*, (B), 26 (1) 33–39.

[27] Avolio, M. V., Crisci, G. M., D'Ambrosio, D., Di Gregorio, S., Iovine, G., Rongo, R., Spataro, W. (2003). An extended notion of cellular automata for surface flows modelling. *WSEAS Trans. Circuits Syst.*, 2 1080–1085.

[28] Avolio, M.V., Lupiano, V., Mazzanti, P., Di Gregorio, S. (2009). A Cellular Automata Model for Flow-like Landslides with Numerical Simulations of Subaerial and Subaqueous Cases. In Wohlgemuth, V., Page, B., Voigt, K. (eds), EnviroInfo 2009, Vol. 1, pp. 131–140, Shaker Verlag GmbH, Aachen.

[29] D'Ambrosio, D., Di Gregorio, S., Iovine, G. (2003). Simulating debris flows through a hexagonal Cellular Automata model: SCIDDICA S3-hex. NHESS 3, 545–559.

[30] Hungr, O.,(1995), A model for the runout analysis of rapid flow slides, debris flows, and avalanches. *Canadian Geotechnical Journal*, 32,610–623.

[31] Marchi, E., Rubatta, A. (1981). Meccanica dei fluidi. Principi e applicazioni. UTET, Torino, 120.

[32] Rouse, H. (1950). Engineering Hydraulics. John Wiley & Sons, Chichester.

[33] Bartelt, P., Christen, M., Gruber, U., and Filaferro, E. (2002). AVAL-1D: An avalanche dynamics program for the practice. Proc., Interpraevent 2002 in the Pacific Rim, Vol. 2, *Int. Res. Soc. Interpraevent for the Pacific Rim*, Matsumoto, Japan, 715–725.

[34] Errera A. (2007). Analisi dei processi fisici nelle valanghe di neve e conseguenze sulla pianificazione territoriale. Applicazione all'area di Davos (CH). MsC Thesis (in Italian). *Dept of Earth Sciences*, University of Milan-Bicocca.

[35] Mellor, M. (1978). Dynamics of snow avalanches. Rockslides and avalanches, 1: Natura phenomena, developments in geotechnical engineering, B. Voight, ed., Vol. 14 *A Elsevier Scientific*, New York, 753–792.

[36] Tai, Y. C., Hutter, K., Gray, J. M. N. T. (2001) Dense granular avalanches: Mathematical description and experimental validation. *Lect. Notes Phys.*, 582, 339–366.

[37] Sovilla, B., Bartelt, P. (2002). Observation and modelling of snow avalanche entrainment. Nat. Hazards Earth Syst. Sci., 2, 169–179.

[38] D'Ambrosio, D., Spataro, W. (2007). Parallel evolutionary modelling of geological processes. Parallel Computing 33 (3), 186–212.

[39] Margreth, S. (2004). Paravalanches et barrieres à neige. Université Européenne d'été sur la neige e les avalanches, Villa Camerun, Courmayeur http://www.obs.ujf-grenoble.fr/risknat/pages/universites/UEE2010/modules/UEE2010-Module8.pdf.